



Geographia Polonica
2025, Volume 98, Issue 4, pp. 523-534
<https://doi.org/10.7163/GPol.0314>



INSTITUTE OF GEOGRAPHY AND SPATIAL ORGANIZATION
POLISH ACADEMY OF SCIENCES
www.igipz.pan.pl

www.geographiapolonica.pl

LICHENS AS AN INDICATOR OF AIR POLLUTION – INTEGRATION OF SEM/EDS AND MACHINE LEARNING METHODS

Mirosław Szwed  • Dariusz Pasieka 

Faculty of Natural Sciences

Jan Kochanowski University of Kielce

Żeromskiego 5, 25-369 Kielce, Poland

e-mails: miroslaw.szwed@ujk.edu.pl (corresponding author) • dariusz.pasieka@ujk.edu.pl

Abstract

Thalli of *Xanthoria parietina* (L.) Th. Fr. lichen collected in locations featuring different pollutant deposit conditions in the urban space of Kielce, including those with intense vehicle traffic, low emission and alkalization from the nearby cement and limestone plant and the open-pit mine were subject to microscopic analyses. The lichen surface had cellular structures with particles characteristic of respective pollutant sources of identified shape and chemical composition (SEM/EDS). The predominant type of particles in the city includes mineral dusts containing silicon and aluminium (natural mineral weathering) and soot with carbon, sulphur and nitrogen (low emission and transport). Sharp-edged structures exceeding 20 μm made of calcium, magnesium and sulphur (cement and lime particles) accompany much smaller, round particles with $\varnothing < 5 \mu\text{m}$ containing iron, aluminium and other heavy metals (industrial fossil fuel combustion). The micrographs taken were used to build a model to create a self-learning pollutant identification system based on the activity of deep neural networks (ResNet). The trained algorithm is able to detect individual items in new micrographs with 71% result. Adding up areas of identified objects (using Euclidean equation) allows identifying their emission sources.

Keywords

lichen • air pollution • Kielce • SEM/EDS • machine learning

Introduction

Lichen belong to a group of popular organisms with properties allowing to diagnose air pollution (Hawksworth & Rose, 1970; De Wit, 1983; Conti & Cecchetti, 2001; Ahmadjian, 1993). Their physiological reactions to identified anthropogenic pressure were confirmed

by numerous works (Takano et al., 2024; Topal et al., 2023). The lichen types used for biomonitoring are analysed as pollution indicators *in situ* (Vitali et al., 2019; Fortuna et al., 2020; Dron et al., 2021) and as transplanted from non-polluted areas (woods, parks, reserves) to degraded areas for specific exposure time to observe organism reactions to pollution (Jia

et al., 2019; Józwiak & Józwiak, 2009). Szwed et al., 2020; Monaci et al., 2022). Common orange lichen *Xanthoria parietina* (L.) Th. Fr. used for the studies is common lichen known for its tolerance to air pollution, including heavy metals. Its thallus is relatively large, with diameter up to 10 cm, usually rosette-shaped, with no soralia and isidia, loosely attached to the substrate, orange and yellow (or greenish and yellow in shaded places). It is a photophilous, calciphile and nitrophilous lichen, common on various substrates, including on fertile deciduous tree and shrub bark. It often grows in large quantities, overgrowing the whole twigs, branches and trunks covered by dust containing calcium carbonate and nitrogen compounds (Fałtynowicz, 2020). The metal-accumulating properties in thalli of common orange lichen were an incentive to use it for biomonitoring (Brunialti & Frati, 2007). It is classified as nitrophilous lichen (Gaio-Oliveira et al., 2004), growing in polluted environment (Rhzaoui et al., 2015; Biřová et al., 2019). According to the 7-point biological scale for epiphyte lichen modified for Polish conditions (Hawksworth & Rose 1970), *Xanthoria parietina* is classified as level 3 – internal zone of reduced vegetation (Kiszka, 1998).

This work demonstrates the opportunity to use micrographs of thalli of *Xanthoria parietina* (L.) Th. Fr. as an input for building the pollutant identification system based on deep neural networks. The model trained based on graphic analysis of pollutants visible in SEM (Scanning Electron Microscope) images is able to segment, convolute and predict them in new images (output). The method employed reduces the time required for comprehensive air quality assessment significantly and offers new opportunities to identify sources of pollution using artificial intelligence. Micrographs of lichen biota have never been utilised before to assess the air pollution level based on machine learning. The novel aspect of this study is the integration of these two approaches: SEM/EDS analysis of lichens as a surface for particle accumulation and the use of neural networks for automatic classification of these particles.

Materials and methods

Study area – city of Kielce

Thalli of epiphyte *Xanthoria parietina* (L.) Th. Fr. were collected in September 2023 in the urban zone of Kielce (20°38'E, 50°53'N) situated in south central Poland (Fig. 1). Samples were taken from deciduous trees, mainly maples (*Acer* sp.) and lindens (*Tilia* sp.), at approximately 1.5 m above ground level, from both trunks and branches. A control sample was collected in Świętokrzyski National Park (30 km from Kielce). The city with the area of 109.45 km² and 175 thousand inhabitants is developed in 21.82% and the housing estates comprise blocks of flats and single family houses (City Hall of Kielce 2025). The meteorological conditions are measured in the station of the Institute of Meteorology and Water Management, National Research Institute, (IMGW-PIB) Kielce-Suków. The hottest month in 2023 was August (average temperature in Kielce was 19.6°C), and the coldest one was February (average temperature in Kielce was 0.6°C). The month with the highest temperature recorded for 24 hours, i.e. 26.3°C, was July. It was 1.1°C higher than the standard one for many years. The total precipitation in 2023 at Kielce-Suków station was 690.8 mm. The highest total precipitation in Kielce was recorded in August, amounting to 90.1 mm. In 2023, the wind blew mostly from the west (> 50% of time in a year). A public health hazard in Kielce is the concentration of benzo(a) pyrene (annual average is 2 ng/m³) included in airborne dust PM10. Increased concentrations of this pollutant were recorded in heating periods (January to March, October to December), with 1 ng/m³ considered to be the permissible value (Annual assessment of air quality in Świętokrzyskie Voivodeship. Voivodeship Report for 2023).

Lichen sampling and preparation

Lichen thallus pieces were collected for analysis from trees in selected locations up to 1.5 m above land level. Next, they were transported to the Laboratory of Environmental Studies at

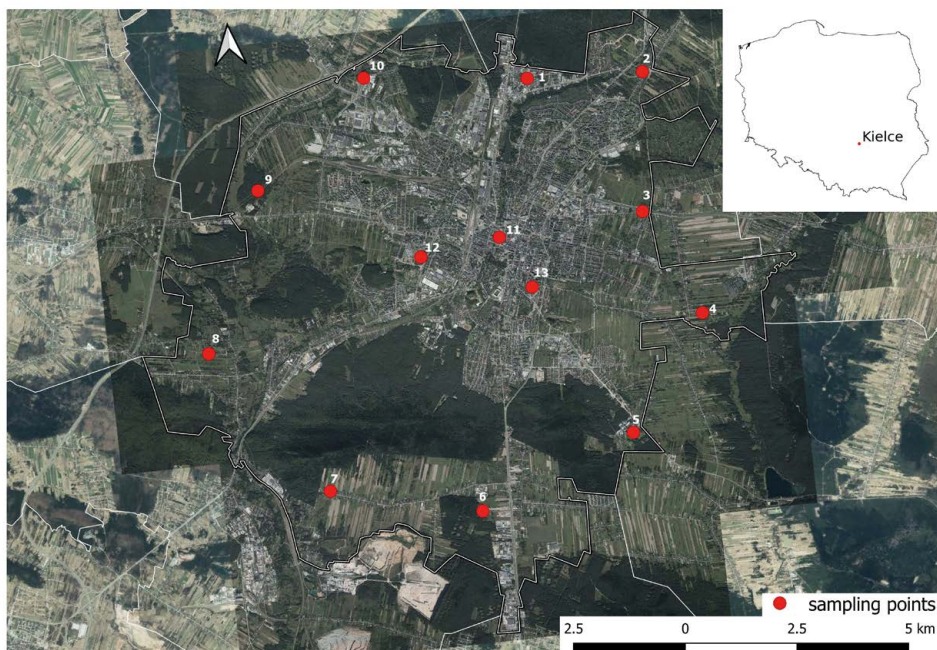


Figure 1. Location of measurement points in Kielce (based on GUGiK orthophotomap)

Jan Kochanowski University of Kielce and subjected to microscopic analyses. The collected material was stuck to \varnothing 12 mm aluminium tables by means of carbon discs. The tables with the samples were placed in the Leica EM SC050 and then sputtered with 24 carat gold in an argon atmosphere with layer thickness control (10 nm) with a quartz crystal microbalance. After the sputtering was completed, the samples were placed in the FEI Quanta 250 electron scanning microscope, and then subjected to EDS (Energy Dispersive Spectroscopy) chemical analysis using the EDAX Genesis analyser (X-ray wavelength spectrometer). The analysis of the surface of lichen from selected locations allowed determining the elemental composition (qualitative analysis) and micronutrient percentage (quantitative analysis) of the deposited particles.

Software and processing

The SEM micrographs in $\times 500$, $\times 1,000$, and $\times 2,000$ magnification were used to identify characteristic urban pollutants visible in

images. The selected items were coloured: red (technogenic spherules), pink (soot), yellow (gypsum and cement particles) and blue (mineral particles). The colourful layers in the images (made in GIMP v. 2.10.38) were the input for self-learning algorithm written in Python. Neural networks using image convolution captured the most important properties and then predicted them in new images based on pixel associations.

Results of the studies

The micrographs taken confirmed significant quantitative diversification of objects deposited on lichen surface. The samples collected from Świętokrzyski National Park were characterised by a much lower share of particles when compared to the urban ones. Hence, reference samples revealed a low share of elements other than carbon and oxygen (C – ca. 40%Wt, O – ca. 30%Wt) characteristic of living organisms. The fine and coarser mineral dusts, technogenic spherules and soot particles, visible in photos of lichen from Kielce,

were present in various proportions. Euclidean equations allowed adding up areas of individual colours ascribed to individual pollution classes in photos processed by Artificial Intelligence (AI) which facilitates interpretation of the obtained results significantly. In micrographs with clear prevalence of pink, soot particles from transport and low emissions are clearly prevalent. The lichen specimens with this pollutant were collected at major traffic arteries and single-family residential estates (city centre and suburbs). Yellow and red (cement and limestone particles and technogenic spherules) were present primarily in photos of lichen from south-western part of the city. Fine mineral particles (blue) were more scattered and were present in all images, with the highest share in the northern part. The SEM/EDS analyses allowed classifying urban pollutants by shape, size, and chemical composition (Fig. 2).

In the pictures of lichen from Świątokrzyski National Park (reference sample), low amount of pollutants was found. The chemical composition of those samples was characteristic of living organisms (with carbon and oxygen). Apart from carbon and oxygen (ca. 40%Wt), the tiny round particles (ca. \varnothing 5 μ m) contained silicon and aluminium (ca. 40%Wt). The share of other elements (including sodium, magnesium, potassium, calcium and iron) did not exceed 3%Wt each. Ellipsoid soot particles ca. 50 μ m (C ca. 70%Wt, O ca. 10%Wt) contained aluminium, silicon, sulphur and calcium ca. 3%Wt each. Small mineral particles were the most abundant, and their edges were rounded, shape irregular and dimensions highly diverse, from 2 to 60 μ m, mostly those containing silicon (up to 50%Wt). Calcium particles (50-60%Wt Ca) with magnesium, manganese and iron had geometrical shapes.

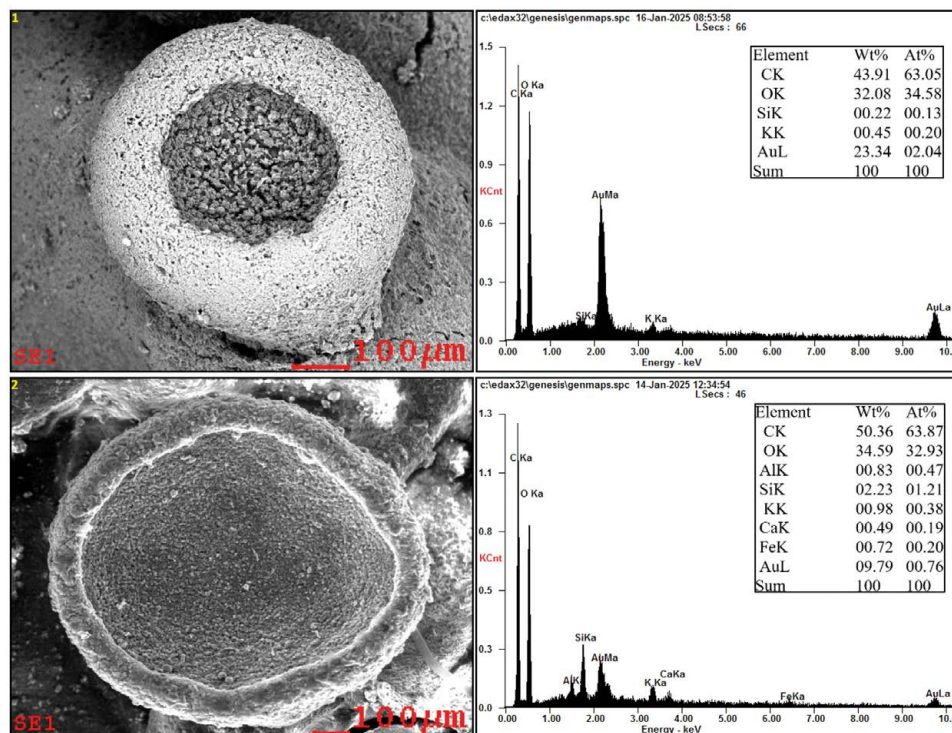


Figure 2. SEM/EDS analysis of the surface of lichens; 1-Lichen from Świątokrzyski National Park (reference sample), 2-Xanthoria parietina, city center (sample no.13), 3-Technogenic spherules (sample no.4), 4-Soot particles (sample no.11), 5- Mineral particles (sample no.2), 6- Calcium particles (sample no.7)

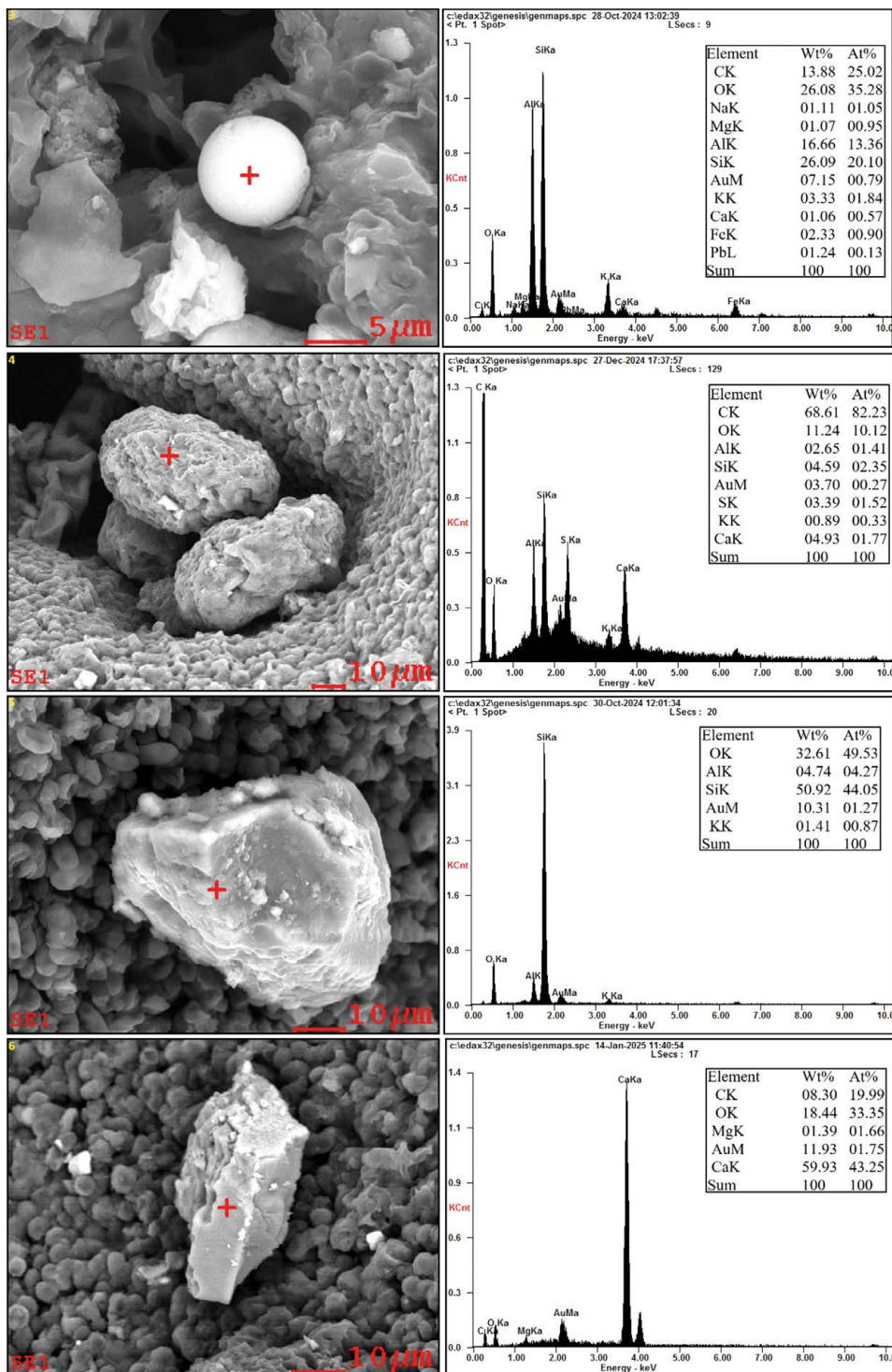


Figure 2. (cd) SEM/EDS analysis of the surface of lichens; 1-Lichen from Świątokrzyski National Park (reference sample), 2-Xanthoria parietina, city center (sample no.13), 3-Technogenic spherules (sample no.4), 4-Soot particles (sample no.11), 5- Mineral particles (sample no.2), 6- Calcium particles (sample no.7)

SEM images taken were analysed by AI to discover properties taught during the training of the developed algorithm. The diagram of its operation is presented in Figure 3. ResNet (Residual Neural Network) is widely used in such tasks as image classification, object detection or segmentation (He et al., 2016), but its use for pollutant segmentation needs modifying. ResNet introduces residual connections which allow effective learning of very deep networks (Li et al., 2024). A key component of ResNet is residual blocks learning just the “difference” (residuum) between input and output which prevents gradient disappearance problem. Standard ResNet was designed to classify (e.g. to ascribe a single label to an image) which means that it needs to be modified in order to operate on pixels (segmentation). The typical steps include removal of a fully connected layer and addition of a decoder (convolution). Similar to U-Net, ResNet uses skip connections between encoder and decoder layers for segmentation which helps retain details at the pixel level (Liu et al., 2024). ResNet acts as an encoder, separating important image properties at various levels of abstraction (edges, textures, shapes). The outcome is a tensor of properties having low resolution, but high level

of abstraction. The decoding (unsampling) part restores image resolution by converting the tensor of properties into prediction for every pixel.

The output is probability maps where every pixel is ascribed to one class. The final layer (sigmoid) ascribes a class to every pixel based on maximum probability. The input for the created model was the training images with colours (masks) imposed for individual pollutants (classes). The expected output was a mask with every pixel classification. The IoU (Intersection over Union) cost functions were used for every class. The trained model is able to scale and normalize new photos (pre-processing), find characteristic properties and recreate new masks anticipating a class for every pixel. To analyse a percentage share of colours in the image, image processing methods based on RGB (Red, Green, Blue) value analysis were used. The number of pixels corresponding to every colour class was calculated based on Euclidean distance (Nda et al. 2016) between the RGB value of a given pixel and the target value for the colour, considering pre-set tolerance ranges (maximum permissible distance between the pixel and the target colour). The result was the total of pixels ascribed to every colour in the mask (Fig. 4).

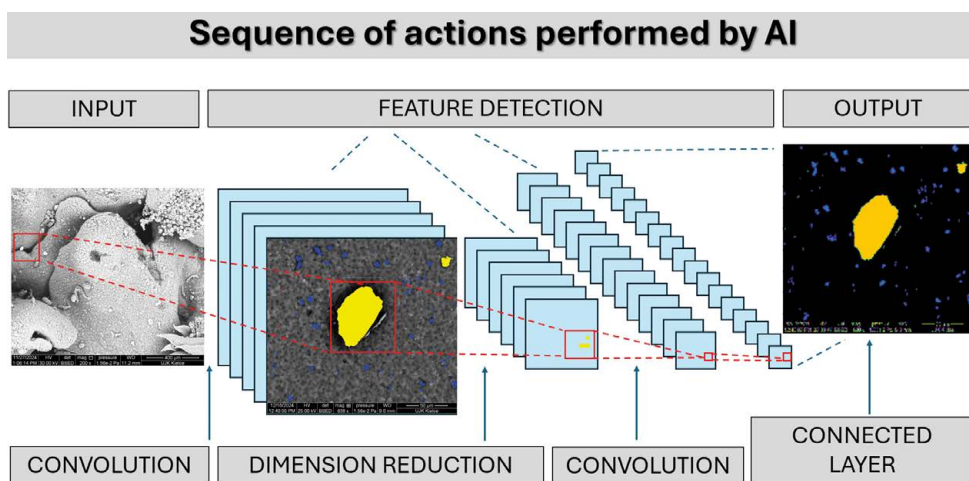


Figure 3. The operation diagram of neural networks for pollutant identification in SEM images of *Xanthoria parietina*

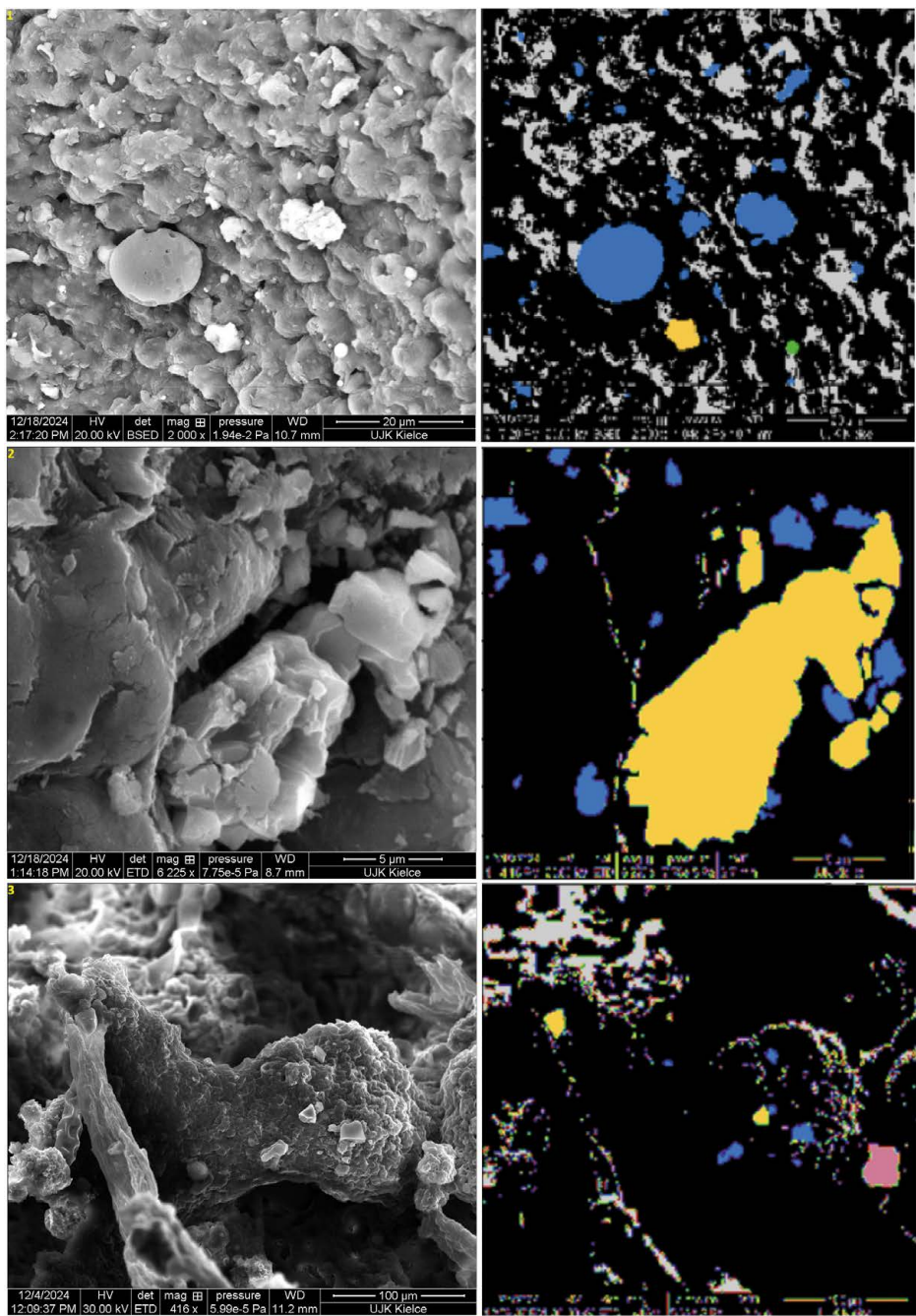


Figure 4. Graphic outcome of the machine algorithm operation 1 – Sample no. 2 (blue: 10.41%, yellow: 5.98%, red: 4.32%, pink: 0.00%), 2 – Sample no. 7 (blue: 10.47%, yellow: 33.63%, red: 1.13%, pink: 0.00%), 3 – Sample from point no. 12 (blue: 3.32%, yellow: 3.76%, red: 2.60%, pink: 15.04%)

Discussion

The results of this study indicate significant differences in the chemical composition of dust deposited on lichens in various parts of the city. Observed mineral particles rich in silicon and aluminum may originate from natural rock weathering processes as well as open-pit mining activities. The dominance of technogenic spherules and soot particles in areas with high traffic and the presence of lime particles near industrial plants confirm the effectiveness of the applied method for identifying emission sources. Urban dust, i.e., air pollution originating from road traffic, industry, building heating, and other urban sources, can be transported over various distances depending on its size, composition, and atmospheric conditions. Larger dust particles ($> 10 \mu\text{m}$, PM10), originating from sources such as roads, tire wear, and brake pad abrasion, settle relatively quickly (Thorpe & Harrison, 2008). Finer particles (PM2.5, PM1), which are produced by the combustion of fuels (e.g., coal, gasoline, diesel), can remain in the atmosphere for days or weeks (Seinfeld & Pandis, 2016). They are typically carried far from the emission source over regional distances (Pöschl, 2005). Ultrafine particles (nanoparticles, soot, sulfate, and nitrate aerosols) remain in the atmosphere the longest and can be transported between continents (Zhang et al., 2015). Academic works describing a biomonitoring use of lichenbiota in areas with diverse anthropogenic pressure focus on the identification of the condition and the chemical composition of individual specimens. Because of the significant geographical distribution of common orange lichen, it was used in many parts of the world. Stable carbon and nitrogen isotopes were analysed in thalli of *Xanthoria parietina* and *Physcia* spp. in Manchester (Niepsch et al., 2023). The authors proved that the recorded loads of carbon, nitrogen and sulphur in lichen and associated signatures of stable isotopes allow identifying urban areas with inferior quality of air. Carbon combustion, road transport and metallurgical industry resulted in higher concentration of lead and iron in common orange

lichen in Morocco (Rhzaoui et al., 2015). The analysis of physiological processes in cells of *Xanthoria parietina* in Zemplínsky Branč (eastern Slovakia) provided information on the possibility to absorb and defend from copper as a result of the secondary metabolite called parietin (Biřová et al., 2019). Physiological parameters (chlorophyll A fluorescence and integrity, content of soluble proteins, ergosterol level) were changed by a higher Cu dose during long-term experiment. In studies carried out in Lublin (Poland), parietin properties relating to protection from cadmium in photobiont cells were analysed (Kalinowska et al., 2015). In thalli of *X. parietina* with no parietin, Cd ions were more toxic in much lower doses of Cd than in intact thalli. The comparison of absorption properties of two species of *Hypogymnia physodes* and *X. parietina* near Tver (Russia) found out that both species absorbed significant amounts of Zn, Mn, Cu, Cd, V and Pb, and that *X. parietina* was highly specific for Sn and Cr absorption, while *H. physodes* for Ni and Co (Meysurova & Notov, 2020). The reach of point emission sources based on the following elements accumulated in thalli of *X. parietina*, i.e. As, Cr, Cu, Fe, Se, V and Zn was reported near Manisa in Turkey (Gür & Yaprak, 2011). Areas polluted with those elements were situated close to a coal-fired power station Soma in spots corresponding to the prevailing direction of wind. *X. parietina* in L'Aquila in Italy recorded even earthquake and rebuilding works (Di Biase et al., 2022).

Biomonitoring studies in Kielce using transplanted *Hypogymnia physodes* Nyl. lichen revealed varied anthropogenic pressure in the city depending on the season of the year, with the cold six months characterised by much higher share of heavy metals (Pb, Cd, Cu and Zn) in lichen thalli which was explained by increased emission of harmful gases and dusts in a heating season. The scanning microscopy allowed identifying also lime particles from the carbonate mining and processing plant to the south west of Kielce on lichen surface (Szwed et al., 2020).

The existing works concerning machine learning application have been based primarily

on the analysis of historical data concerning pollutant concentration and meteorological conditions used to anticipate future pollution (Ayus et al., 2023; Lei et al., 2024). Based on the analysis of available data, neural networks are able to calculate pollution level which will occur soon (Czernecki et al., 2021). There are also known automated methods to identify lichen based on photos (Presta et al. 2020) or segmentation of cellular image micrographs (Abdallah et al., 2020). The application of neural networks to identify pollutants on *Pinus sylvestris* L. needles was described in papers (Szwed & Pasięka, 2024; Szwed et al., 2024). In the presented method, the lichen micrographs serve not only to detect pollutants but also to identify sources of pollution by calculating the total percentage share of a given colour in the generated images. The adopted solutions are highly effective (71%) and their effectiveness can be improved. If the predominant colour in the generated image is yellow (the highest percentage share calculated using Euclidean equation), the dust is emitted primarily by the cement and limestone plant. If it is pink, i.e. when the predominant particles in the generated image of lichen collected near traffic routes and single-family housing estates are soot ones, they are emitted by combustion engines and fossil fuel burning. Small mineral particles (blue) observed in the northern part of the city may come not only from natural weathering of aluminosilicates but also from the open-pit mine of quartz sandstone in nearby Wiśniówka (Migaszewski et al., 2007). Compared to previous studies (Niepsch et al., 2023; Meysurova & Notov, 2020), the method used in this study allows not only for determining chemical composition but also for the rapid processing of large image datasets and automatic pollutant identification. The integration of SEM/EDS with AI enables potential use in monitoring seasonal changes in dust deposition. A crucial question remains whether this method is relevant only on a local scale or can be adapted to other areas with similar pollution characteristics. In this context, preliminary studies on dust characteristics for each examined area may be necessary.

Summary

In urban space, there are diverse dust pollutants and their sources to be found. Identification of harmful particles using Artificial Intelligence and SEM/EDS micrograph analysis on the surface of a popular bioindicator is an alternative to automatic metering stations. The integration of SEM/EDS and machine learning methods contributes to the advancement of AI-driven air quality assessment using lichens as bioindicators. The presented method of detecting the pre-trained objects is a universal tool and will surely be developed. Its basic advantage is a low analysis cost and high effectiveness. Another advantage is the possibility to identify pollutant sources by adding up shares of individual classes on the surface of images generated by AI.

Acknowledgments

This research was funded by grants awarded by the Head of the Jan Kochanowski University of Kielce, numbers SUPB.RN.24.107

Authors' contribution

MS: Writing – review & editing, Writing – original draft, Visualization, Software, Project administration, Methodology, Investigation, Formal analysis, Data curation.

DP: Supervision, Software, Methodology, Data curation.

Declaration of competing interest

The authors declare that they have no known competing financial interests or personal relationships that could have appeared to influence the work reported in this paper.

Data Availability Statement

The data presented in this study are available on request from the corresponding author.

Editors' note:

Unless otherwise stated, the sources of tables and figures are the authors', on the basis of their own research.

References

- Abdallah, H., Formosa, B., Liyanaarachchi, A., Saigh, M., Silvers, S., Arslanturk, S., ... & Gatti, D. L. (2020). Res-CR-Net, a residual network with a novel architecture optimized for the semantic segmentation of microscopy images. *Machine Learning Science and Technology*, 1(4), 045004. <https://doi.org/10.1088/2632-2153/aba8e8>
- Ahmadjian, V. (1993). *The Lichen Symbiosis*. John Wiley & Sons.
- Ayus, I., Natarajan, N., & Gupta, D. (2023). Comparison of machine learning and deep learning techniques for the prediction of air pollution: A case study from China. *Asian Journal of Atmospheric Environment*, 17(1). <https://doi.org/10.1007/s44273-023-00005-w>
- Biľová, I., Gaga, M., & Backor, M. (2019). Physiological responses of *Xanthoria parietina* to longterm copper excess: Role of the extracellular secondary metabolite parietin. *Botanica Serbica*, 43(2), 133-142. <https://doi.org/10.2298/botserb1902133b>
- Brunialti, G., & Frati, L. (2007). Biomonitoring of nine elements by the lichen *Xanthoria parietina* in Adriatic Italy: A retrospective study over a 7-year time span. *The Science of the Total Environment*, 387(1-3), 289-300. <https://doi.org/10.1016/j.scitotenv.2007.06.033>
- Conti, M., & Cecchetti, G. (2001). Biological monitoring: lichens as bioindicators of air pollution assessment – a review. *Environmental Pollution*, 114(3), 471-492. [https://doi.org/10.1016/s0269-7491\(00\)00224-4](https://doi.org/10.1016/s0269-7491(00)00224-4)
- Czernecki, B., Marosz, M., & Jędruszkiewicz, J. (2021). Assessment of machine learning algorithms in short-term forecasting of PM10 and PM2.5 concentrations in selected Polish agglomerations. *Aerosol and Air Quality Research*, 21(7), 200586. <https://doi.org/10.4209/aaqr.200586>
- De Wit, T. (1983). Lichens as indicators for air quality. In *Springer eBooks* (pp. 273-282). https://doi.org/10.1007/978-94-009-6322-1_10
- Di Biase, L., Di Lisio, P., Pace, L., Arrizza, L., & Fattorini, S. (2022). Use of Lichens to Evaluate the Impact of Post-Earthquake Reconstruction Activities on Air Quality: A Case Study from the City of L'Aquila. *Biology*, 11(8), 1199. <https://doi.org/10.3390/biology11081199>
- Dron, J., Ratier, A., Austruy, A., Revenko, G., Chaspoul, F., & Wafo, E. (2021). Effects of meteorological conditions and topography on the bioaccumulation of PAHs and metal elements by native lichen (*Xanthoria parietina*). *Journal of Environmental Sciences*, 109, 193-205. <https://doi.org/10.1016/j.jes.2021.03.045>
- Fałtynowicz, W. (2020). *Porosty: Przewodnik do rozpoznawania gatunków na drzewach przydrożnych*. Stowarzyszenie Eko-Inicjatyw.
- Fortuna, L., Incerti, G., Da Re, D., Mazzilis, D., & Tretiach, M. (2020). Validation of particulate dispersion models by native lichens as point receptors: A case study from NE Italy. *Environmental Science and Pollution Research*, 27(12), 13384-13395. <https://doi.org/10.1007/s11356-020-07859-5>
- Gaio-Oliveira, G., Dahlman, L., Palmqvist, K., Martins-Loução, M. A., & Máguas, C. (2004). Nitrogen uptake in relation to excess supply and its effects on the lichens *Evernia prunastri* (L.) Ach and *Xanthoria parietina* (L.). *Planta*, 220(5), 794-803. <https://doi.org/10.1007/s00425-004-1396-1>
- GUGiK. Head Office of Geodesy and Cartography. <https://www.gov.pl/web/gugik>
- Gür, F., & Yaprak, G. (2011). Biomonitoring of metals in the vicinity of Soma coal-fired power plant in western Anatolia, Turkey using the epiphytic lichen, *Xanthoria parietina*. *Journal of Environmental Science and Health Part A*, 46(13), 1503-1511. <https://doi.org/10.1080/10978526.2011.609075>
- Hawksworth, D. L., & Rose, F. (1970). Qualitative scale for estimating sulphur dioxide air pollution in England and Wales using epiphytic lichens. *Nature*, 227(5254), 145-148. <https://doi.org/10.1038/227145a0>
- He, K., Zhang, X., Ren, S., & Sun, J. (2016). Deep Residual Learning for Image Recognition. In *2016 IEEE Conference on Computer Vision and Pattern Recognition (CVPR)* (pp. 770-778). Las Vegas, NV, USA, 2016. <https://doi.org/10.1109/CVPR.2016.90>

- IMGW-PIB Kielce-Suków. Institute of Meteorology and Water Management National Research Institute. <https://imgw.pl/>
- Jia, S., Zhang, X., Liu, Q., Chen, Q., Li, X., Pang, X., Li, J., Wu, Q., Zhao, L., & Liu, H. (2019). Spatial-Temporal Patterns of Element Concentrations in *Xanthoparmelia camtschadalis* Transplanted along Roads. *Polish Journal of Environmental Studies*, 29(1), 121-129. <https://doi.org/10.15244/pjoes/99905>
- Jóźwiak, M., & Jóźwiak, M. (2009). Influence of cement industry on accumulation of heavy metals in bioindicators. *Ecological Chemistry and Engineering S*, 16(3), 323-334.
- Kalinowska, R., Bačkor, M., & Pawlik-Skowrońska, B. (2015). Parietin in the tolerant lichen *Xanthoria parietina* (L.) Th. Fr. increases protection of *Trebouxia* photobionts from cadmium excess. *Ecological Indicators*, 58, 132-138. <https://doi.org/10.1016/j.ecolind.2015.05.055>
- Kiszka, J. (1998). Lichen flora as indicative of the environmental degradation in the Czarna Wisetka and Biała Wisetka catchments. *Studia Naturae*, 44, 53-71.
- Lei, T. M. T., Cai, J., Molla, A. H., Kurniawan, T. A., & Kong, S. S. (2024). Evaluation of machine learning models in air pollution prediction for a case study of Macau as an effort to comply with UN sustainable development goals. *Sustainability*, 16(17), 7477. <https://doi.org/10.3390/su16177477>
- Li, H., Hussin, N., He, D., Geng, Z., & Li, S. (2024). Design of image segmentation model based on residual connection and feature fusion. *PLoS ONE*, 19(10), e0309434. <https://doi.org/10.1371/journal.pone.0309434>
- Liu, S., Wu, C., Xu, F., Chi, J., Yu, X., & Wei, L. (2024). RPNET: a Residual Pyramid Semantic Segmentation network based on Atrous convolution. In *2022 34th Chinese Control and Decision Conference (CCDC)*, 1624-1629. <https://doi.org/10.1109/ccdc62350.2024.10588154>
- Meysurova, A. F., & Notov, A. A. (2020). Estimated indicator ability of several lichens for ecological monitoring of metals using atomic emission spectral analysis. *Journal of Applied Spectroscopy*, 87(1), 83-91. <https://doi.org/10.1007/s10812-020-00967-7>
- Migaszewski, Z., Starnawska, E., & Gałuszka, A. (2007). Gorceixite from the Upper Cambrian Rocks of the podwiśniówka Mine Pit, Holy Cross Mountains (South-Central Poland). *Mineralogia*, 38(2), 171-184. <https://doi.org/10.2478/v10002-007-0025-6>
- Monaci, F., Ancora, S., Paoli, L., Loppi, S., & Wania, F. (2022). Lichen transplants as indicators of gaseous elemental mercury concentrations. *Environmental Pollution*, 313, 120189. <https://doi.org/10.1016/j.envpol.2022.120189>
- Nda, M., Amadou, T., Dossa, A., & Gouton, P. (2016). Choice of distance metrics for RGB color image analysis. *Electronic Imaging*, 28, 1-4. <https://doi.org/10.2352/ISSN.2470-1173.2016.20.COLOR-349>
- Niepsch, D., Clarke, L. J., Newton, J., Tzoulas, K., & Cavan, G. (2023). High spatial resolution assessment of air quality in urban centres using lichen carbon, nitrogen and sulfur contents and stable-isotope-ratio signatures. *Environmental Science and Pollution Research*, 30(20), 58731-58754. <https://doi.org/10.1007/s11356-023-26652-8>
- Pöschl, U. (2005). Atmospheric aerosols: Composition, transformation, climate and health effects. *Angewandte Chemie International Edition*, 44(46), 7520-7540. <https://doi.org/10.1002/anie.200501122>
- Presta, A., Pellegrino, F. A., & Martellos, S. (2021). Learning-based automatic classification of lichens from images. *Biosystems Engineering*, 213, 119-132. <https://doi.org/10.1016/j.biosystemseng.2021.11.023>
- Rhzaoui, G. E., Divakar, P. K., Crespo, A., Tahiri, H., & Alaoui-Faris, F. E. E. (2015). *Xanthoria parietina* as a biomonitor of airborne heavy metal pollution in forest sites in the North East of Morocco. *Lazaroa*, 36, 31-41. https://doi.org/10.5209/rev_laza.2015.v36.49487
- Roczna ocena jakości powietrza w województwie świętokrzyskim. Raport wojewódzki za rok 2023. (2023). Główny Inspektorat Ochrony Środowiska w Kielcach. <https://powietrze.gios.gov.pl/pjp/rwms/publications/card/2009>
- Seinfeld, J. H., & Pandis, S. N. (2016). Atmospheric chemistry and physics: From air pollution to climate change (3rd ed.). John Wiley & Sons.

- Szwed, M., Kozłowski, R., & Żukowski, W. (2020). Assessment of air quality in the South-Western part of the Świętokrzyskie Mountains based on selected indicators. *Forests*, 11(5), 499. <https://doi.org/10.3390/f11050499>
- Szwed, M., & Pasieka, D. (2024). Micrographic image of air pollutants in Poland. *Archives of Environmental Protection*, 50(4), 3-8. <https://doi.org/10.24425/aep.2024.152890>
- Szwed, M., Żukowski, W., & Pasieka, D. (2024). Air pollution rapid assessment tool with the use of pine needles: A machine learning approach. *Sylwan*, 168(11), 835-845. <https://doi.org/10.26202/sylwan.2024056>
- Takano, A. P. C., Rybak, J., & Veras, M. M. (2024). Bioindicators and human biomarkers as alternative approaches for cost-effective assessment of air pollution exposure. *Frontiers in Environmental Engineering*, 3. <https://doi.org/10.3389/fenve.2024.1346863>
- Thorpe, A., & Harrison, R. M. (2008). Sources and properties of non-exhaust particulate matter from road traffic: A review. *The Science of the Total Environment*, 400(1-3), 270-282. <https://doi.org/10.1016/j.scitotenv.2008.06.007>
- Topal, E. I. A., Topal, M., Öbek, E., & Aslan, A. (2023). Lichens as Biomonitors of Air Pollutants Deposition: Strategically important element pollution. *Bitlis Eren Üniversitesi Fen Bilimleri Dergisi*, 12(2), 485-495. <https://doi.org/10.17798/bitlisfen.1243631>
- Urząd Miasta Kielce. <https://www.kielce.eu>
- Vitali, M., Antonucci, A., Owczarek, M., Guidotti, M., Astolfi, M. L., Manigrasso, ... & Protano, C. (2019). Air quality assessment in different environmental scenarios by the determination of typical heavy metals and Persistent Organic Pollutants in native lichen *Xanthoria parietina*. *Environmental Pollution*, 254, 113013. <https://doi.org/10.1016/j.envpol.2019.113013>
- Zhang, R., Wang, G., Guo, S., Zamora, M. L., Ying, Q., Lin, Y., ... & Wang, Y. (2015). Formation of urban fine particulate matter. *Chemical Reviews*, 115(10), 3803-3855. <https://doi.org/10.1021/acs.chemrev.5b00067>